Interlaminar Fracture Toughness of Woven Fabric Composite Laminates with Carbon Nanotube/Epoxy Interleaf Films

Ryan J. Sager,[1] Patrick J. Klein,[1] Daniel C. Davis,[1] Dimitris C. Lagoudas,[1] Graham L. Warren,[2] Hung-Jue Sue[2]

[1]*Department of Aerospace Engineering, Texas A&M University, College Station, Texas 77843-3141*
[2]*Department of Mechanical Engineering, Texas A&M University, College Station, Texas 77843-3123*

Received 1 June 2010; accepted 29 September 2010
DOI 10.1002/app.33479
Published online 21 March 2011 in Wiley Online Library (wileyonlinelibrary.com).

ABSTRACT: The Mode I interlaminar fracture behavior of woven carbon fiber/epoxy composite laminates incorporating partially cured carbon nanotube/epoxy composite films has been investigated. Laminates with films containing carbon nanotubes (CNTs) in the as-received state and functionalized with polyamidoamine were evaluated, as well as laminates with neat epoxy films. Double-cantilever beam (DCB) specimens were used to measure G_{Ic}, the critical strain energy release rate (fracture toughness) versus crack length. Post-fracture microscopic inspection of the fracture surfaces was performed. Results show that initial fracture toughness was improved with the amino-functionalized CNT/epoxy interleaf films, but the important factor appears to be the polyamidoamine functionalization, not the CNTs. The initial fracture toughness remained relatively unaffected with the incorporation of neat epoxy and as-received CNT/epoxy interleaf films. Plateau fracture toughness was unchanged with the use of functionalized CNT/epoxy interleaf films, and was reduced with the use of neat epoxy and as-received CNT/epoxy interleaf films. © 2011 Wiley Periodicals, Inc. J Appl Polym Sci 121: 2394–2405, 2011

Key words: fracture; composites; nanocomposites; carbon nanotubes; films

INTRODUCTION

Woven fabric carbon/epoxy composites have been embraced by the aerospace, automotive, and sporting goods industries due to their high in-plane specific strength and stiffness. However, like other laminate materials, they are most vulnerable to out-of-plane loading, often failing in delamination. Efforts to improve the interlaminar strength of laminate composites have met with some success, including 3-D reinforcement and improvements in the toughness of the matrix through additives.

Through-thickness reinforcement through 3-D weaving and Z-pinning has shown promising gains in interlaminar toughness; however due to damage caused to the reinforcing fibers from the weaving process, as well as through the insertion of the Z-pins, in-plane properties are reduced.[1] Most successful attempts to improve the toughness of the matrix have focused on the addition of modifiers to the matrix such as thermoplastic resins, rubbers, and particles. However, the addition of thermoplastics and rubbers may result in significant degradation of the matrix properties, such as strength, stiffness and glass transition temperature.[2]

The high specific stiffness, strength, and electrical and thermal conductivity of carbon nanotubes (CNTs) make them a promising reinforcement for creating multifunctional composite materials with electrical and/or thermal functionality. Additionally, the small size and high aspect ratio of CNTs make them an ideal filler material, with the potential to significantly enhance bulk material properties when mixed with resins even at low weight fractions. These improvements include greater resin toughness and stiffness, as well as increased electrical and thermal conductivity.[3–5] One of the greatest difficulties in using CNTs as reinforcement in composites is dispersing them uniformly within the matrix. Because of their high surface area and large aspect ratios, unmodified CNTs have a strong tendency to agglomerate, resulting in poor dispersion in the matrix. Conventional methods of dispersion, such as sonication, are only effective on small batches of material due to the extreme reduction in vibrational energy with increasing distance from the sonic tip,[3] thus making large scale mixing of

Correspondence to: P. J. Klein (pjklein@aeromail.tamu.edu).

Contract grant sponsor: Air Force Research Laboratory, Minority Leaders Program; contract grant number: F33601-05-D-1912.

nanotubes both difficult and time consuming. Surface modification, especially through functionalization, has led to improvements in the ability to disperse CNTs throughout a matrix. Functionalization has also been shown to increase the bond strength between the CNTs and the matrix.[5,6] The combination of good CNT-matrix adhesion, dispersion, and an entanglement effect of embedded nanotubes within the matrix have been attributed to increased fracture toughness values of the bulk material by up to 18% over neat epoxy with only 0.1 wt % amino-functionalized double-wall carbon nanotubes (DWCNT) and a 26% increase in fracture toughness using only 1.0 wt % functionalized DWCNTs.[3] Similarly, tensile strength and Young's modulus were also improved with the addition of functionalized CNTs.[3]

Although effective methods of dispersing CNTs in resins have been developed, incorporation of CNT-modified resins into fiber-reinforced composites poses challenges. Traditional resin infusion techniques such as resin transfer molding (RTM) and vacuum-assisted resin transfer molding (VARTM) can result in nonuniform dispersion of CNTs in composite panels due to a filtering effect of the reinforcing fiber, especially when using untreated CNTs.[7,8] Therefore, a procedure that can effectively introduce the CNTs into the laminate without the need to flow a CNT-modified resin would be advantageous. Three techniques for introducing CNTs into laminates have been reported in the literature: (1) by growing CNTs directly on the fabric using chemical vapor deposition (CVD),[9,10] (2) by spraying solvent-borne CNTs onto the fabric surface,[11,12] and (3) by applying a mixture of uncured resin ("a-stage" thermoset) and CNTs to the surface.[13] An alternative technique that offers some advantages, which is the focus of this work, is to incorporate CNTs into the laminate through the use of interleaved b-staged (i.e., partially cured) CNT-modified epoxy films.[14] The interleave film technique has been used to improve the interlaminar fracture toughness and impact resistance of laminate composites.[15–19] The interleaf film technique offers several advantages over the previously discussed techniques for introducing CNTs into the laminate structure. Unlike CNT growth by CVD, when producing actual composite parts and structures, the interleaf film can be applied over large areas, or on large pieces of fabric that would not fit in a CVD chamber. In contrast to spraying techniques, the dispersion of the CNTs in a film is maintained once the CNTs are introduced into the laminate. Furthermore, the films can be applied only where needed in the structure, reducing manufacturing expense.

The significance of the thickness and ductility of the resin-rich interlaminar region to interlaminar fracture toughness had been noted by Bradley and Cohen.[20] Typical interleave films are relatively ductile fully cured thermosets or thermoplastics which toughen the laminate by allowing development of a plastic zone ahead of the crack tip, and have sufficient thickness to greatly reduce or eliminate constraint of the plastic zone by adjacent fiber reinforcement.[20] Although usually used in prepreg lamination techniques that use a hot press, interleave films can be used in a resin transfer lamination process such as VARTM. The interleave film technique allows specific placement of the CNT-modified resin within the composite laminate only where it is needed. In this work, the interleave films use the same epoxy that is used for the laminate matrix, because it was desired to eliminate an abrupt, and potentially weak, interface between the laminate matrix and the film resin, a problem observed by Ozdil and Carlsson[17] for some films. Furthermore, because the interleave epoxy initially has a low degree of cure (i.e., crosslinking), it will essentially melt at the panel curing temperatures, facilitating penetration of the CNT-rich resin into the fiber layers and assimilation by the infused epoxy resin. The goal is for the b-staged interleave film to essentially cease to exist as a distinct interlaminar layer, and instead create a layer of toughened CNT-rich resin that interpenetrates and bridges the adjacent fiber reinforcement layers, with a thickness comparable to interlaminar regions in noninterleaved areas. By not significantly increasing the interlaminar resin thickness, significant reduction in laminate modulus should be avoided. During curing of the laminate, the laminate matrix and the interleave film will achieve the same, full degree of crosslinking, and the only difference between the CNT-rich epoxy and the matrix epoxy will be the presence of the functionalized CNTs.

In addition to the potential toughening benefit provided by the CNTs, the incorporation of an interlaminar, CNT modified epoxy layer, or layers, could also provide additional benefits in out-of-plane thermal and electrical conductivity, creating truly multi-functional composite materials. This potential for a multifunctional benefit was a major factor in choosing to investigate CNTs as a resin modifier over other materials. The combination of outstanding mechanical properties along with exceptional electrical and thermal conductivities is not available in any other material. In aerospace applications, achieving metal-like electrical and thermal conductivities in high-specific-strength and high-toughness composites would have great benefits. Although other additives or reinforcements may offer greater potential for the improvement of fracture toughness, none offer the unique multifunctional capabilities of CNTs.

In this research, we have investigated the Mode I interlaminar fracture behavior of woven carbon fiber-epoxy laminates fabricated using vacuum-assisted

TABLE I
Fiber and Matrix Properties

Property	Hexcel IM7	EPON 862/W
Density (g/cm^3)	1.79	1.2
Tensile Modulus (GPa)	276	2.72
Tensile Strength (MPa)	5480	78

TABLE II
Interleave Film Properties

CNT Type	CNT wt %	T_g (°C)	Thickness (μm)
Neat Epoxy	0	38.1	28
As-Received	0.5	45.6	43
Functionalized 1	0.5	36.2	122
Functionalized 2	0.5	>36.2	137

resin transfer molding that have been reinforced with CNTs by the incorporation of thin, b-staged CNT-epoxy nanocomposite interleaf films. Double-cantilever beam (DCB) specimens are used for the measurement of G_{Ic} , the critical strain energy release rate (fracture toughness) and the generation of resistance curves. Postfracture microscopic inspection of the fracture surfaces is performed to determine crack paths and crack morphology. The films used in this study were fabricated at the Polymer Technology Center of Texas A&M University, using the process detailed by Warren et al.[14]

EXPERIMENTAL SETUP

The laminates under investigation were fabricated from 20 layers of satin weave carbon fiber fabric, using EPON 862 epoxy resin and EPIKURE W curing agent, with a single b-staged (partially-cured) EPON 862/W nanocomposite interleaf film at the mid-plane. EPON 862 is a difunctional bisphenol-F epoxide (diglycidyl ether of bisphenol-F). EPIKURE W curing agent is an aromatic diamine (diethyltoluenediamine). The carbon fiber fabric is a Hexcel four-harness satin weave of IM7 fiber (SGP203), with identical warp and fills yarns of 6K filament count. IM7 fiber is an intermediate modulus, PAN-based carbon fiber commonly used in the aerospace industry. The fiber and resin properties from the manufacturer's data sheets are summarized in Table I.[21,22] Symmetric laminates were laid up with the yarns aligned with the panel length and width directions. The stacking sequence is such that the direction of the yarns facing the panel mid-plane alternate between 0 and 90 degrees to the ultimate direction of crack growth, with the yarns immediately adjacent to the mid-plane being parallel to the direction of crack growth. A pre-existing crack was created at one edge of the laminate by incorporating a 12.5 μm FEP film at the mid-plane during lamination.

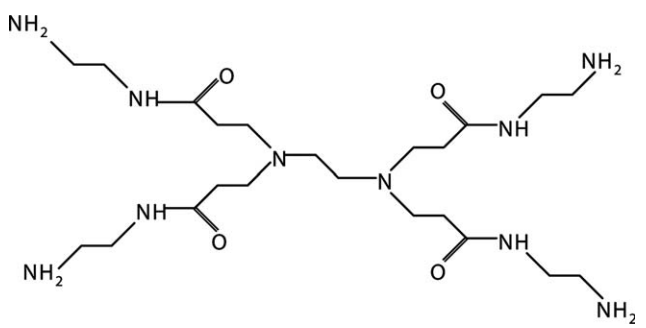

Figure 1 Schematic of PAMAM-0.

Laminate panels were fabricated incorporating a single b-staged (partially cured) EPON 862/W interleaf film at the mid-plane. One of three different types of film was used: with either as-received CNTs or functionalized CNTs, and a neat epoxy film, each explained further below. One each of panels using the as-received CNT and neat films were fabricated, and two panels were fabricated using the functionalized CNT films. For the control, four panels without any film were fabricated, hereafter referred to as "standard" panels.

The b-staged interleaf films were fabricated at the Polymer Technology Center (PTC) at Texas A and M University. To produce the films, XD-grade CNTs (Carbon Nanotechnologies, Inc.) were incorporated into bulk EPON 862/W to produce two separate XD CNT/epoxy mixtures, with either amino-functionalized or untreated (as-received) XD-CNTs. XD-CNTs are mixture of single-walled, double-walled, and multi-walled CNTs, which also contain graphite, amorphous carbon, and iron catalyst contaminates. Amine functionalization of the CNTs was performed first by oxidation of the surface, with subsequent reaction of polyamidoamine generation-0 (PAMAM-0) dendrimers to the oxidation sites. PAMAM-0 is a branched polymer with a molecular weight of 517, with four terminal amine groups giving it a functionality of 8. A schematic of PAMAM-0 is shown in Figure 1. Functionalization of the CNTs as well as their incorporation into the bulk resin to produce the CNT/epoxy mixtures followed the procedures outlined by Warren et al.[14] Once the CNT-modified resins had been produced, thin epoxy interleaf films were cast onto release-coated paper using a modified Elcometer 4340 automatic film applicator. The thin films were then cured to a 50% degree of cure. All CNT modified films contained 0.5 wt % XD grade CNTs and ranged in thickness from 28 to 137 μm. The properties of all films used are shown in Table II. The glass transition temperatures (T_g) were determined by differential scanning calorimetry (DSC).

The laminates were fabricated using a heated vacuum-assisted resin transfer molding process (H-VARTM) developed by Bolick and Kelkar[23] at North

TABLE III
Tested Panels

Panel film type	Panels tested	Specimens tested
Standard (no film)	4	20
Neat Epoxy	1	5
Epoxy/As-received CNTs	1	5
Epoxy/Functionalized CNTs	2	10

Carolina A and T University, whereby a glass plate mold is heated by a temperature-controlled heating pad placed underneath. The stack of fabric reinforcement is held against the mold with two vacuum bags (and inner bag and an outer bag) sealed to the mold, and the heated resin is infused into the reinforcement stack using atmospheric pressure. The H-VARTM set-up is shown in Figure 2. The bottom surface of the glass plate mold is maintained at 65°C during resin infusion. The resin reservoir is maintained at 50°C during the infusion, and is infused at a rate of approximately 6 mm per minute. The completed panels averaged 55% fiber volume fraction with an average thickness of 4.4 mm.

EXPERIMENTAL PROCEDURE

Specimen dimensions and the test parameters were in compliance with ASTM Test Method D 5528.[24] The DCB fracture specimens were 170 mm long and 25 mm wide. A tested DCB specimen is shown in Figure 3. Hinged loading tabs (cut from aluminum piano hinge) were bonded to the outer faces of the specimens at the cracked end using an epoxy paste adhesive, with the loading point nominally 25 mm from the end of the specimen, giving a nominal initial crack length of approximately 51 mm. The edges of the specimen were painted with a white spray enamel primer to improve the visibility of the

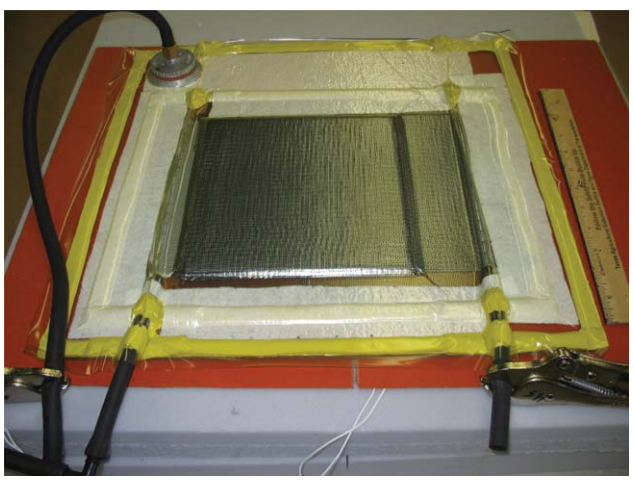

Figure 2 Heated vacuum-assisted resin transfer molding set-up. [Color figure can be viewed in the online issue, which is available at www.wileyonlinelibrary.com.]

Figure 3 Tested laminate DCB specimen. [Color figure can be viewed in the online issue, which is available at www.wileyonlinelibrary.com.]

crack tip. To provide a means of measuring the crack length, a scale printed on a self-adhesive label was applied to the painted edge of the specimen. After the specimen was loaded into the test frame grips, the position of the scale zero point relative to the loading points was measured using a video camcorder mounted on a translatable stage. During the test, the crack advancement was videotaped. In this way, the crack length prior to each instance of crack growth could be measured by replaying the videotape. The timing of the video and data collection were easily correlated.

The specimens were loaded on a 100 k*N* capacity MTS servo-hydraulic load frame in displacement control at a rate of 3.0 mm/min. The specimens were unloaded after the initial crack advancement, and also after the second crack advancement. This procedure would help to ensure that fracture toughness data was obtained starting at the end of the film if the initial observed crack growth was not actually from the end of the film. In most cases, the second measured toughness value would be from the first "sharp" crack, with minimal fiber bridging.

Data reduction to obtain G_{Ic} , the critical strain energy release rate, or fracture toughness, is based on the compliance calibration method proposed by Berry,[25] and suggested in ASTM D 5528. The specimen compliance, C (the ratio of load point displacement to load, δ/P) can be expressed as

$$C = \frac{a^n}{H} \tag{1}$$

where a is the crack length, and, for an ideal specimen, $n = 3$ and $H = 3/2EI$, where E is the specimen tensile modulus, and I is the moment of inertia of the specimen cross section. The compliance, C, of the specimens is determined for each crack length from the peak load before crack propagation, P_c, and the corresponding critical displacement, δ_c. The exponent n in Eq. (1) is equivalent to the slope the plot of log C versus log a. In practice, the value of n will be less than the ideal value of three, because the beam is not perfectly built, and thus rotation may occur at the delamination front. The fracture

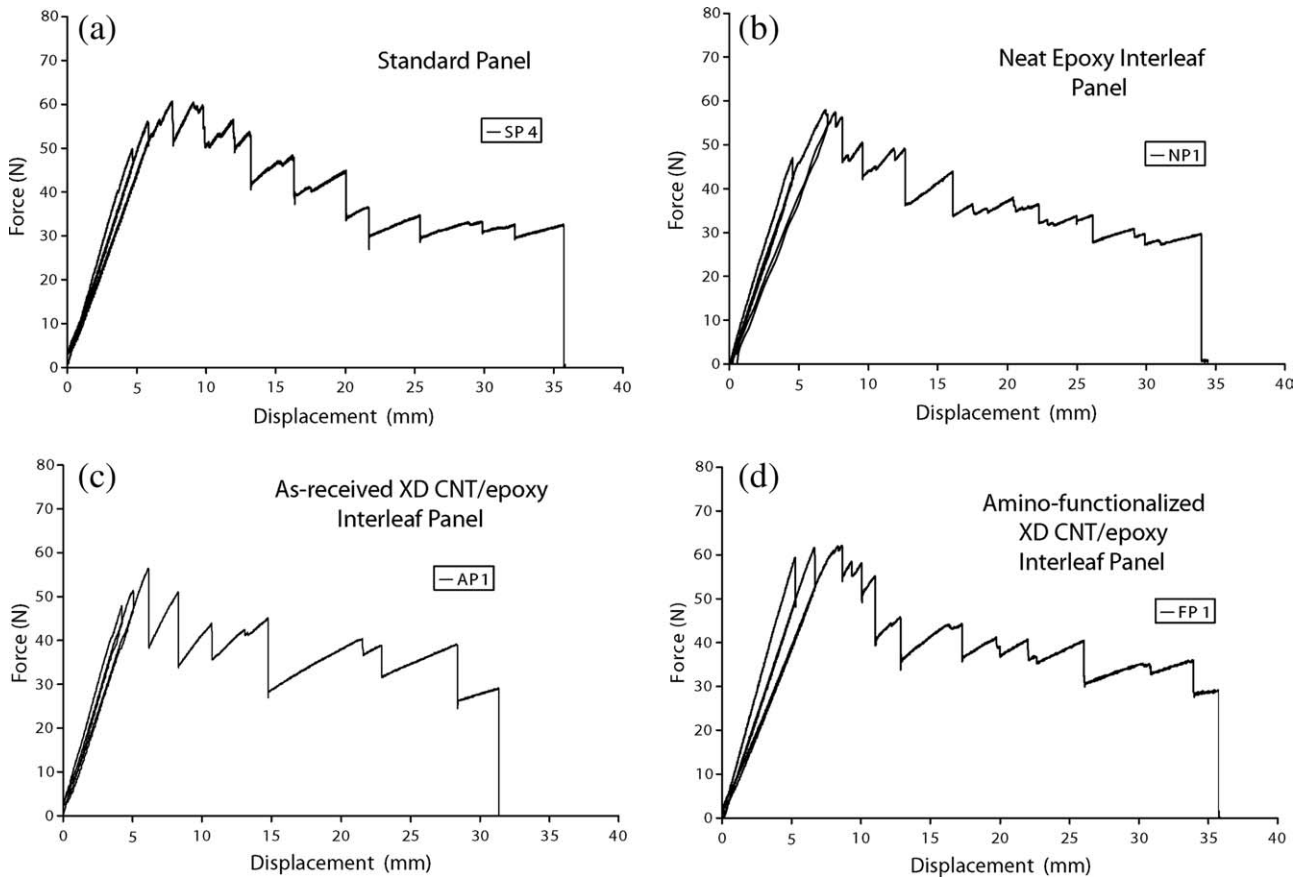

Figure 4 Typical load-displacement curves for DCB specimens: (a) standard panels; (b) neat epoxy interleaf panel; (c) as-received XD CNT interleaf panel; (d) amino-functionalized XD CNT interleaf panels.

toughness, G_{Ic}, at each crack length, a, can be determined from the expression

$$G_{Ic} = \frac{nP_c\delta_c}{2wa} \quad (2)$$

where w is the specimen width.

RESULTS

Fracture toughness

Table III lists the number of panels tested of each film type, and the total number of specimens tested of each film type. Five specimens each from the standard, neat, as-received, and functionalized XD CNT film panels were tested. Figure 4 shows the typical load-displacement (P - δ) curves for each panel type tested. Initial response for all specimens was linear, indicating elastic loading, followed by a small but sudden decrease in load. Visible crack propagation was observed simultaneously with the decrease in load. In all specimens, an increase in load was then observed after which larger sudden decreases in load occurred throughout the remainder of the tests. This saw-toothed response is commonly observed in woven composites and is characterized by a stick-slip behavior as the crack is arrested by the fiber microstructure until sufficient load is again achieved to further propagate the crack.[26–31] Further toughening is achieved through fiber bridging behind the crack tip and was seen throughout the specimens tested. Fiber bridging occurs when fibers from the bounding layers fail to separate as the crack progresses, thereby bridging the crack gap. This crack bridging mechanism serves to further accentuate the unstable, large drops in load demonstrated in the saw-tooth nature of the P - δ curves. The initial small load decrease observed at the initial crack length is indicative of the initial crack propagating from the crack starter film within the matrix up to the fiber microstructure where it is arrested.

Interlaminar fracture toughness values were calculated from the peak loads, and the corresponding displacement, just prior to crack propagation using Eq. (2). The value of n used in Eq. (2) was determined for each specimen, and ranged from 2.66 to 2.91, with an average of 2.77 across all panels. Typical delamination crack growth resistance curves (R-curves) for all panels (one specimen per panel) are shown in Figure 5. The delamination resistance generally increased over the initial 5 mm before

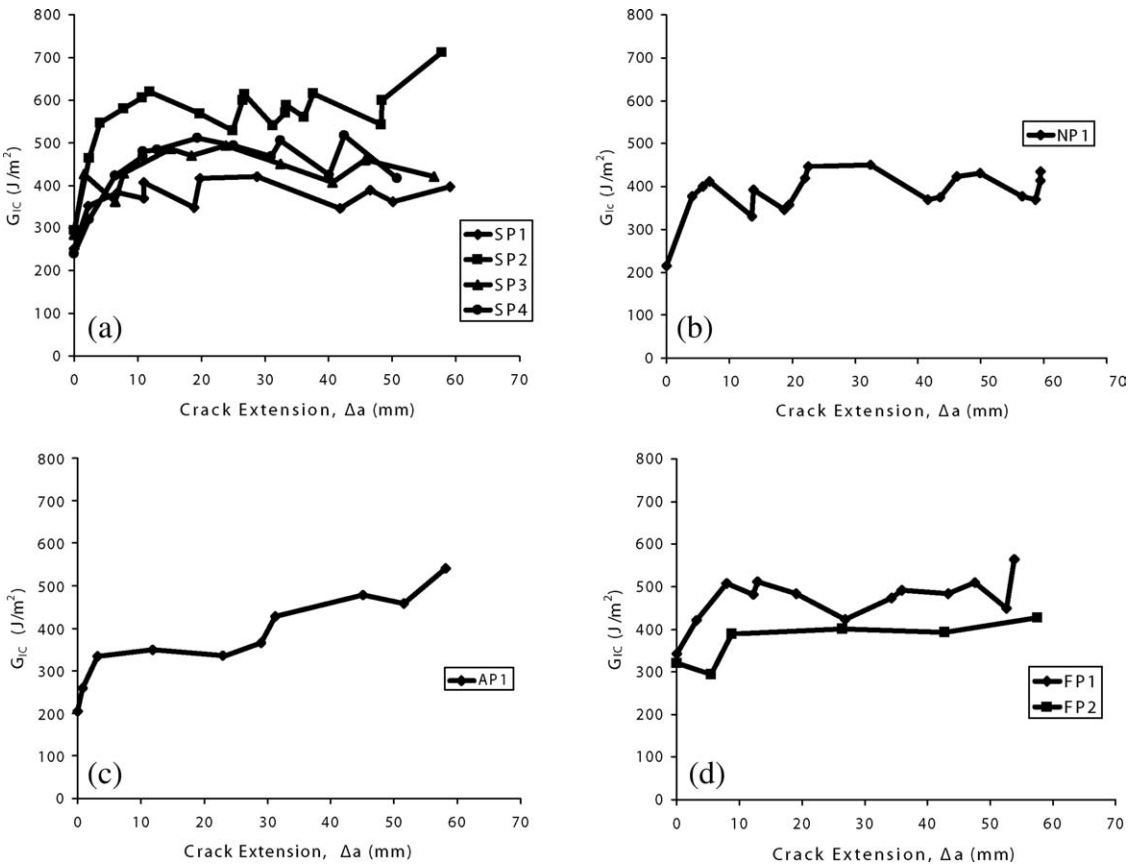

Figure 5 Typical R-curves for DCB specimens (one from each panel): (a) standard panels; (b) neat epoxy interleaf panel; (c) as-received XD CNT interleaf panel; (d) amino-functionalized XD CNT interleaf panels.

reaching a plateau region. This behavior is due to the effect of fibers bridging the crack as it grows, acting to support more load. The large amount of scatter in the data is typical of a woven fabric composite, and is attributable to the variation in microstructure due to the fabric weave as the crack tip advances as well as the effect of fiber/ply bridging.[28] In Figure 6, the average G_{Ic} of all specimens for each panel type is plotted versus *a*. The plots show more clearly the differences in initial fracture toughness and plateau fracture toughness for the different panel types.

Figure 7 shows the average initial Mode I G_{Ic} values for each panel type, with the error bars showing the 95% confidence intervals. The average initial G_{Ic} for the standard panels was 249 J/m^2, which is comparable with results from similar materials in other studies.[27] The large degree of variation of the

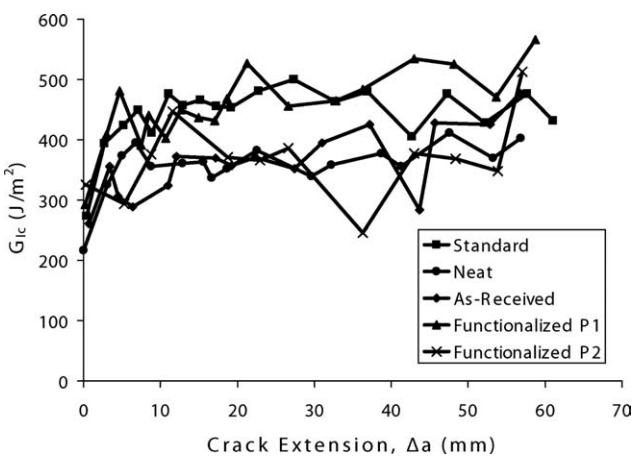

Figure 6 Panel average R-curves.

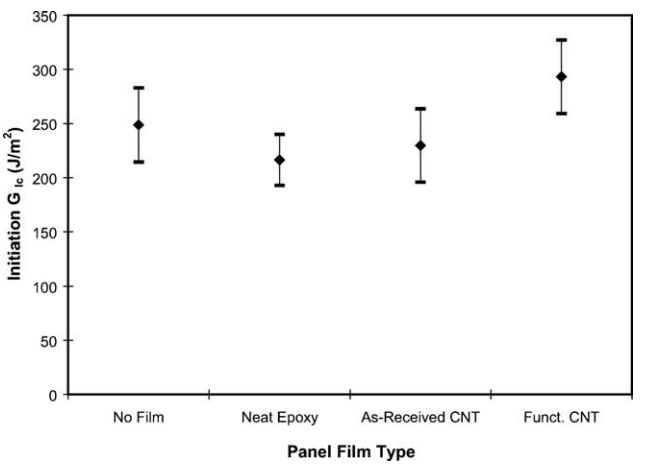

Figure 7 Initiation fracture toughness vs. film type.

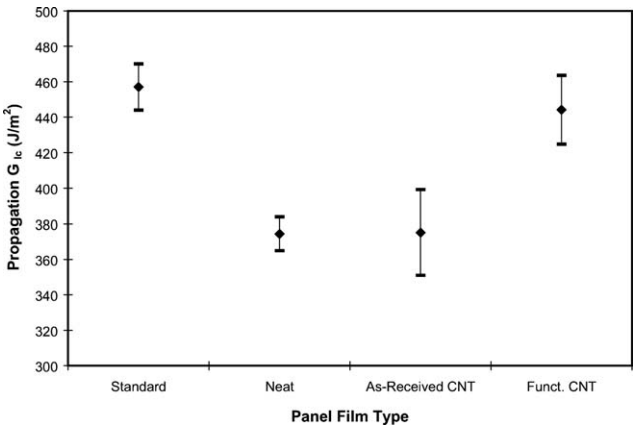

Figure 8 Propagation fracture toughness vs. film type.

initial toughness values within a panel type is not uncommon, and has been attributed by Martin to the variation of the position of the end of the crack starter insert with respect to fiber yarns.[27,28,31] The average initial G_{Ic} for the neat epoxy interleaved panel was 216 J/m^2, a 13% reduction with respect to the standard (noninterleaved) panels. The average initial G_{Ic} for the as-received XD CNT/epoxy interleaved panel was 230 J/m^2 which was 8% lower than the noninterleaved panels, and only 6% higher than the neat epoxy interleaved panel, indicating that the as-received XD CNTs had little, if any, effect. The functionalized XD CNT/epoxy interleaved panels produced the highest initial fracture toughness with an average value of 293 J/m^2, 18% higher than the noninterleaved panels and 36% higher than the neat epoxy interleaved panel. These results for the interleaved panels are similar to the results for the bulk fracture toughness of the film materials observed by Warren et al.[14] Warren et al. fabricated bulk specimens of the film material using the same process and facilities used in this study, and demonstrated no increase in fracture toughness (K_{Ic}) for 0.5 wt % as-received XD CNT/epoxy nanocomposites compared to neat EPON 862/W. However, for PAMAM-0 functionalized XD CNT/epoxy nanocomposites, they observed an increase of 19% in K_{Ic} over neat epoxy. Warren et al. also showed a 146% increase in elongation for the PAMAM-0 functionalized XD CNT/epoxy nanocomposites, relative to the neat epoxy, which suggests that increased plastic work within the plastic zone ahead of the crack tip was the reason for the increased fracture toughness. The increase in toughness observed by Warren et al. in the bulk nanocomposites is comparable to the 18 and 36% increases in initial G_{Ic} of the functionalized panels with respect to the standard and neat interleaved panels in this study. Initial crack growth does not involve fiber bridging, so the initial fracture toughness is more directly related to matrix/film toughness; therefore, the strong correlation between the laminate initial fracture toughness and the bulk nanocomposite fracture toughness is to be expected. There was a significant difference in the initial fracture toughness of the two functionalized-CNT panels, with the second panel having an average toughness 16% higher than

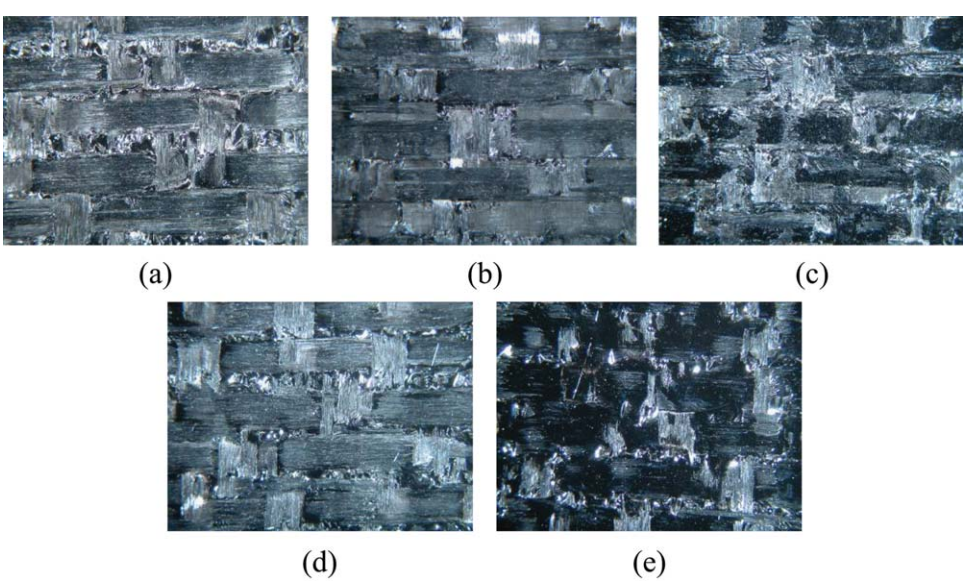

Figure 9 Representative failure surfaces for various panels: (a) standard panels; (b) neat epoxy interleaved panel; (c) as-received XD CNT/epoxy interleaved panel; (d) amino-functionalized XD CNT/epoxy interleaved panel 1; (e) amino-functionalized XD CNT/epoxy interleaved panel 2. [Color figure can be viewed in the online issue, which is available at www.wileyonlinelibrary.com.]

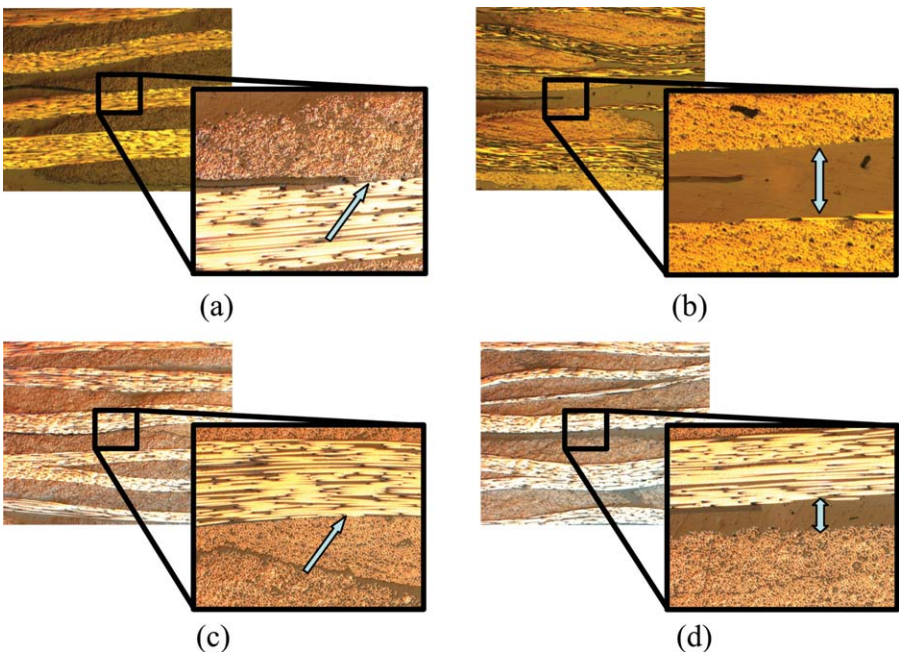

Figure 10 Cross-sections of interleaved panels: (a) functionalized panel 1; (b) neat interleaf panel; (c) as-received CNT panel; (d) functionalized panel 2. [Color figure can be viewed in the online issue, which is available at www.wileyonlinelibrary.com.]

the first. As can be seen in Figure 10, the second functionalized panel had a significantly thicker mid-plane epoxy layer than the first, which would allow development of a larger plastic zone ahead of the crack tip, explaining the higher initial fracture toughness of the second panel.

Figure 8 shows the average plateau Mode I G_{Ic} values for all the panels, with the error bars showing the 95% confidence intervals. The average plateau G_{Ic} for the standard panels was calculated as 459 J/m^2. The average plateau G_{Ic} for the neat epoxy interleaved panel was calculated as 375 J/m^2, an 18% reduction with respect to the noninterleaved panels. The average plateau G_{Ic} for the as-received XD CNT/epoxy interleaved panel was 380 J/m^2, a decrease of 17% relative to the noninterleaved panels. The functionalized XD CNT produced the highest plateau fracture toughness of the interleaved panels with an average value of 438 J/m^2. This demonstrates a decrease in plateau fracture toughness of 5% with respect to noninterleaved panels, and an increase of 17% over the neat epoxy interleaved panel.

Although the plateau fracture toughness for the standard and functionalized XD CNT/epoxy interleaved panels were roughly equal, on average, there is a significant decrease in the plateau fracture toughness for both the neat epoxy and as-received XD CNT/epoxy interleaved panels. This difference is due to the differences in the location of the fracture within the laminate microstructure, as well as in the amount of fiber bridging present within each specimen, seen in Figure 9.

Fracture morphology

Two modes of failure were generally observed on the DCB fracture surfaces. These failure modes are characterized as either "adhesive" failure or "cohesive" failure. Adhesive failure describes failure of the interface, or adhesive bond, between the carbon fiber yarns and the epoxy matrix. Although on a microscopic scale, the failure is necessarily a combination of failure of the fiber/matrix interface and failure of the interfiber resin, macroscopically, it can be described as interfacial failure at the yarn/matrix interface. In contrast, cohesive failure is failure entirely within the matrix, with no direct interaction with the fiber reinforcement.

In the standard panels [Fig. 9(a)], the mode of failure was primarily adhesive, although cohesive failure was necessarily present in the areas between yarns (within a fabric layer), as well as in the crevices where yarns crossover. The adhesive failure must necessarily follow along the undulating surface of the woven fabric. As the crack tip follows the fabric surface, it deviates from a path perfectly parallel with the panel mid-plane, resulting in a Mode II component of failure, which would tend to increase the measured macroscopic Mode I toughness. Additionally, failure was not restricted to the interface between the yarn and the interlaminar matrix. Failure often extended

into the yarns, resulting in fibers being pulled out from the yarns. These pulled out fibers effectively bridge the crack behind the crack tip, supporting load, and thus act as a toughening mechanism.

The fracture surfaces from the neat film panel [Fig. 9(b)] were very similar in appearance to those from the standard panel, with adhesive failure being the primary mode of failure, and having even less intralaminar cohesive failure. Since the composition of the film is identical to the bulk resin, once it is melted during heating in VARTM process, good integration into the laminate is expected, and confirmed in Figure 10(b). Although the failure mode was essentially entirely adhesive, fiber bridging was not as prevalent and severe as in the standard panels, which explains the lower measured fracture toughness relative to the standard panels. Thus, while the film was well integrated into the laminate, it did have a significant detrimental effect on the fiber bridging toughening mechanism, resulting in an 18% decrease in the average plateau fracture toughness relative to the standard panels.

In contrast to the standard and neat film panels, the as-received CNT film panel [Fig. 9(c)] exhibited mostly cohesive failure, in the range of 65 to 75% cohesive, and thus much less fiber bridging. The reason for this appears to be the presence of a thicker interlaminar resin layer at the mid-plane [Fig. 10(c)], allowing the crack to propagate through the resin without the degree of interaction with the fabric layers seen in the standard and neat film panels. There are two film properties that would affect the thickness of the interlaminar resin layer: initial film thickness and the resin melt viscosity. The thickness of the as-received film is 43 μm, or over 50% thicker than the neat epoxy film. The final relative viscosities of the films can be judged from their glass transition temperatures. The neat epoxy film and the functionalized CNT film of the first functionalized panel ("FP 1") have glass transition temperatures of 38.1°C and 36.2°C, respectively. The as-received CNT film has a T_g of 45.6°C, at least 7.5°C higher than the other films. The glass transition temperature is a measure of the degree of crosslinking, which is directly correlated to viscosity, so a film with a higher T_g will have a higher melt viscosity, all other things being equal. The higher viscosity of the as-received CNT film would tend to reduce the amount of resin that is forced into the adjacent fabric layers during the VARTM process, thus increasing the interlaminar resin layer thickness. As shown by the initial fracture toughness results, confirmed by the results of Warren et al.,[14] the toughness of the as-received CNT film was no greater than neat resin. A crack propagating through a layer of as-received CNT modified resin, without any fiber bridging, would be expected to exhibit the low fracture toughness observed.

Like the as-received CNT film panel, the second functionalized CNT film panel [Fig. 9(e)] exhibited mostly cohesive failure, approaching virtually 100% cohesive failure. Again, the factors at work appear to be the initial film thickness and the film melt viscosity, resulting in the thicker interlaminar resin layer shown in Figure 10(d). At 137 μm, the initial thicknesses of the second functionalized CNT film was much greater than the neat epoxy and as-received CNT films, by a factor of four and three, respectively. As with the as-received film, the melt viscosity of the second functionalized film was likely increased relative with that of the neat epoxy film due to a higher degree of crosslinking. Although the T_g of the functionalized CNT films was measured at 36.2°C (slightly lower than the neat epoxy film), the second functionalized film was not used until 3 days after it was fabricated (2 days after the T_g was measured). Since it was stored at room temperature during this time, some additional crosslinking would have occurred, resulting in a higher viscosity. Since the T_g was not measured again just before use, the change is not known, although it was necessary to increase the temperature of the film transfer process by 10°C to get above the glass transition temperature and successfully transfer the film to the fabric layer. Because of the virtually 100% cohesive failure, essentially no fiber bridging occurred in the second functionalized CNT panel, resulting in an average plateau fracture toughness of 374 J/m^2, significantly lower than the standard panels, and roughly equal to the toughness of the neat epoxy film panels and the as-received CNT film panels, despite the presence of the tougher functionalized CNT resin. This suggests that the thickness of the interlaminar resin layer, although greater than intended, was insufficient to allow development of a plastic zone large enough to overcome the loss of the fiber bridging toughening mechanism. The loss of fiber bridging in the second functionalized panel thus reduced the average plateau fracture toughness for the two functionalized panels.

In contrast to the second functionalized film panel, the first functionalized film panel [Fig. 9(d)] exhibited mostly adhesive failure, with a significant amount of fiber bridging. As indicated in the discussion of the second functionalized CNT film above, the viscosity of the first functionalized CNT film was likely lower than both the second functionalized film and the as-received CNT film. The lower viscosity would result in a thinner mid-plane interlaminar resin layer, confirmed in Figure 10(a), resulting in more interaction of the crack with the fabric. Despite the presence of the tougher functionalized CNT film,

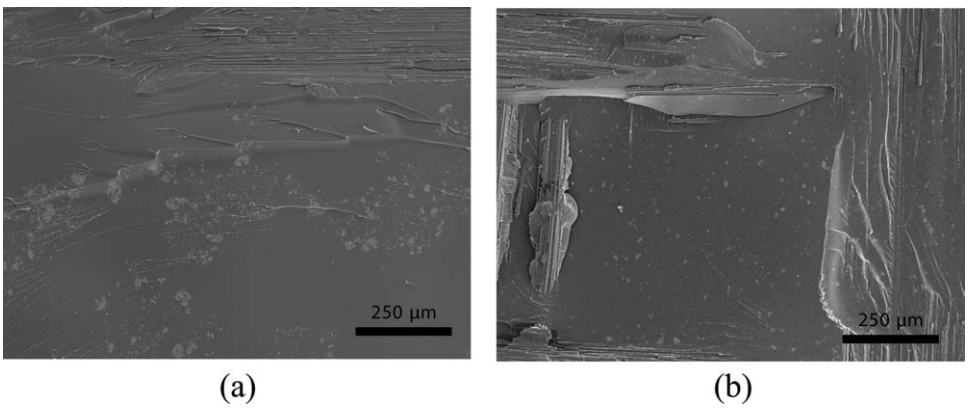

Figure 11 SEM images indicating good coverage of CNTs over the entire fracture surface of CNT-modified interleaf panels: (a) as-received XD CNT; (b) amino-functionalized XD CNT.

the toughness of the first functionalized CNT film panel was not significantly higher than that of the standard panels, indicating that the toughening effect of the functionalization is limited due to constraint of the plastic zone and is overshadowed by the toughening effect of the fiber bridging.

SEM images were taken of the fracture surfaces for the as-received and functionalized XD CNT-modified interleaf film panels to both determine if the CNTs remained in the area of initial placement and to what effect functionalization of the CNTs had on their dispersion. Images were obtained using a JEOL 6400 scanning electron microscope. The presence of CNTs on the fracture surface of the laminates can clearly be seen in Figure 11. These images indicate that the nanotubes remain within the midplane interlaminar region, validating the interleaf method of CNT placement within standard laminate composites. Additionally, the presence of the CNTs along the fracture surface indicates that the crack propagated in the presence of CNTs. Figure 12 shows the difference in dispersion of CNTs within

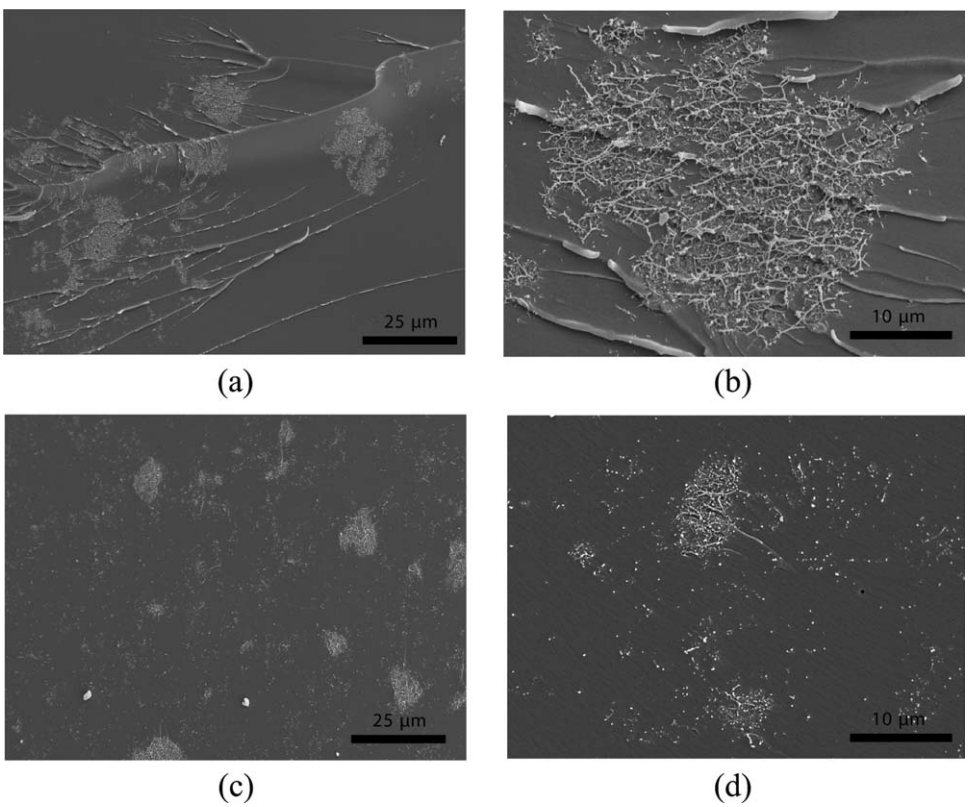

Figure 12 SEM images of fracture surfaces for CNT-modified epoxy interleaf panels: (a) as-received XD CNT, poor dispersion; (b) as-received XD CNT, enlarged region from (a); (c) amino-functionalized XD CNT, good dispersion; (d) amino-functionalized XD CNT, enlarged region from (c).

the interleaf films due to the surface functionalization. The functionalization of the CNTs with PAMAM-0 dendrimer has a clear impact on the dispersion of CNTs within the epoxy interleaf film. The as-received CNT-modified film [Fig. 12(a,b)] demonstrates poor dispersion with large agglomerations and there is little evidence of nanotubes within the epoxy which is not contained within the large agglomerates. The functionalized CNT-modified film [Fig. 12(c,d)], although still exhibiting agglomeration, demonstrates smaller agglomerates than the as-received panel, as well as a greater number of CNTs dispersed individually or in bundles throughout the matrix. Although individual nanotubes by themselves would not be observable at the magnifications shown, the sputtered Au-Pd coating applied to the specimen surfaces could account for at least 60 nm of the 100 nm diameter features, so some of those features could be individual multi-wall CNTs. Furthermore, Sun et al.[32] performed TEM analysis on bulk EPON 862 nanocomposites with the same PAMAM-0 functionalized CNTs (1 wt %), manufactured using the same procedures and facilities, and showed well-dispersed individual and bundled CNTs. The reduced agglomeration and better dispersion of the functionalized CNTs would lead to a more uniform distribution of properties throughout the interleaf film, possibly providing a more consistent mechanical, thermal, and electrical response than a more agglomerated film. Additionally, Gojny et al.[5] have demonstrated that large agglomerations of CNTs within epoxy matrices act as defects, becoming initiation points of failure and therefore possibly producing weaker composite materials. With the addition of functionalization resulting in a better dispersed and less agglomerated concentration of CNTs, the potential of the reinforcing material to become a liability is reduced.

CONCLUSIONS

The effect of XD CNT modified epoxy interleaf films on the Mode I fracture toughness of woven fabric carbon fiber/epoxy composites was examined and compared to results obtained for noninterleaved standard panels, as well as panels modified with neat epoxy interleaf films. The initial fracture toughness of panels containing the neat epoxy and as-received XD CNT interleaf films showed no statistically significant difference with respect to the noninterleaved standard panels. Functionalized XD CNT/epoxy interleaved panels demonstrated an average 18% increase in initial G_{Ic} over standard panels, and a 36% increase over the neat epoxy interleaved panel. The plateau fracture toughness of the functionalized XD CNT/epoxy interleaved panels remained essentially unchanged relative to the standard panels, while the neat and as-received XD CNT/epoxy interleaved panels decreased by 18 and 17% compared to the standard panels, respectively. The decrease in plateau fracture toughness in panels fabricated without the functionalized CNTs is attributed to both the inherently lower toughness of the resin and a suppression of fiber bridging. The presence of large amounts of CNTs along the fracture surface, revealed by SEM, indicates that the use of CNT-modified epoxy interleaf films is an effective method for the controlled placement of CNTs within a laminate composite system. Additionally, the use of functionalization had a positive effect on the dispersion of CNTs within the laminates. This improvement in CNT dispersion would tend to enhance any improvement in the electrical and thermal conductivity of the laminates due to the CNTs, although this aspect was not investigated in this work.

References

1. Lee, L.; Rudov-Clark, S.; Mouritz, A. P.; Bannister, M. K.; Herszberg, I. Compos Struct 2002, 57, 405.
2. Deng, S.; Rosso, P.; Ye, L.; Friedrich, K. Solid State Phenom 2007, 121, 1403.
3. Gojny, F. H.; Wichmann, M. H. G.; Köpke, U.; Fiedler, B.; Schulte, K. Compos Sci Technol 2004, 64, 2363.
4. Awasthi, K.; Awasthi, S.; Srivastava, A.; Kamalakaran, R.; Talapatra, S.; Ajayan, P. M.; Srivastava, O. N. Nanotechnology 2006, 17, 5417.
5. Gojny, F. H.; Schulte, K. Compos Sci Technol 2004, 64, 2303.
6. Gojny, F. H.; Nastalczyk, J.; Zbiginew, R.; Schulte, K. Chem Phys Lett 2003, 370, 820.
7. Sadeghian, R.; Gangireddya, S.; Minaieb, B.; Hsiao, K. T. Compos A 2006, 37, 1787.
8. Fan, Z.; Hsiao, K. T.; Advani, S. G. Carbon 2004, 42, 871.
9. Veedu, V. P.; Cao, A.; Li, X.; Ma, K.; Soldano, C.; Kar, S.; Ajayan, P. M.; Ghasemi-Nejhad, M. N. Nat Mater 2005, 5, 457.
10. Wicks, S. S.; Guzman de Villoria, R.; Wardle, B. L. Compos Sci Technol 2010, 70, 20.
11. Thakre, P. R.; Lagoudas, D. C.; Zhu, J.; Barrera, E. V.; Gates, T. S. Processing and Characterization of Carbon-Fabric/Epoxy Composites, Newport, Rhode Island, 2006.
12. Zhu, J.; Imam, A.; Crane, R.; Lozano, K.; Khabashesku, V. N.; Barrera, E. V. Compos Sci Technol 2007, 67, 1509.
13. Adhikari, K.; Hubert, P.; Simard, B.; Johnston, A. Effect of the Localized Application of SWNT Modified Epoxy on the Interlaminar Shear Strength of Carbon Fibre Laminates, Newport, Rhode Island, 2006.
14. Warren, G. L.; Sun, L.; Hadjiev, V. G.; Davis, D.; Lagoudas, D.; Sue, H. J. J Appl Polym Sci 2009, 112, 290.
15. Masters, J. E. Key Eng Mat 1989, 37, 317.
16. Ishai, O.; Rosenthal, H.; Sela, N.; Drukker, E. Composites 1988, 19, 49.
17. Ozdil, F.; Carlsson, L. A. J Compos Mater 1992, 26, 432.
18. Xuefeng, A. N.; Shuangying, J. I.; Bangming, T.; Zilong, Z.; Xiao-Su, Y. J Mater Sci Lett 2002, 21, 1763.
19. Singh, S.; Partridge, I. K. Compos Sci Technol 1995, 55, 319.
20. Bradley, W. L.; Cohen, R. N. In Delamination and Debonding of Materials, ASTM Special Technical Publication 876; Johnson, W. S., Ed.; American Society for Testing and Materials: Philadelphia, Pennsylvania, 1985; p 389.

21. Product Data Sheet HS-CP-5000, Hexcel Composites, Stamford, Connecticut 2007.
22. Product Data Sheet SC:1183-02, Resolution Performance Products, LLC, Houston, Texas 2002.
23. Bolick, R. L.; Kelkar, A. D. Innovative composite processing by using H-VARTM method, Paris, 2007.
24. ASTM Standard.Standard Test Method for Mode I Interlaminar Fracture Toughness of Unidirectional Fiber-Reinforced Polymer Matrix Composites, ASTM Standard D 5528; ASTM International: West Conshohocken, Pennsylvania, 2001.
25. Berry, J. P. J Appl Phys 1963, 34, 62.
26. Mouritz, A. P.; Baini, C.; Herszberg, I. Compos A 1999, 30, 859.
27. Paris, I.; Minguet, P. J.; O'Brien, T. K. In Composite Materials: Testing and Design, ASTM Special Technical Publication 1436; Bakis, C. E., Ed.; ASTM International: West Conshohocken, Pennsylvania, 2003; Vol. 14, pp 372–390.
28. Alif, N.; Carlsson, L. A.; Gillespie, J. W. In Composite Materials: Testing and Design, ASTM Special Technical Publication 1242; Hooper, S. J., Ed.; American Society for Testing and Materials: West Conshohocken, Pennsylvania, 1997; Vol. 13, pp 82–106.
29. Alif, N.; Carlsson, L. A.; Boogh, L. Compos B 1998, 29, 603.
30. Hansen, P.; Martin, R. DCB, 4ENF and MMB delamination characterisation of S2/8552 and IM7/8552. Technical Report N68171-98-M-5177, Materials Engineering Research Laboratory Ltd. (MERL), Hertford, United Kingdom, 1999.
31. Martin, R.H. J Compos Tech Res 1997, 19, 20.
32. Sun, L.; Warren, G. L.; O'Reilly, J. Y.; Everett, W. N.; Lee, S. M.; Davis, D.; Lagoudas, D.; Sue, H. J. Carbon 2008, 46, 320.